Higher Dispersion Efficacy of Functionalized Carbon Nanotubes in Chemical and Biological Environments

Elena Heister,[†,⊥] Constanze Lamprecht,[‡] Vera Neves,[†,⊥] Carmen Tîlmaciu,[§] Lucien Datas,[§] Emmanuel Flahaut,[§] Brigitte Soula,[§] Peter Hinterdorfer,[‡] Helen M. Coley,[†] S. Ravi P. Silva,[⊥] and Johnjoe McFadden[†,*]

[†]Faculty of Health and Medical Sciences, University of Surrey, Guildford, GU2 7XH, U.K., [‡]Institute of Biophysics, Johannes Kepler University, Altenberger Strasse 69, A-4040 Linz, Austria, [§]Université de Toulouse, UPS/INP/CNRS, Institut Carnot CIRIMAT, 118 route de Narbonne, 31062 Toulouse, Cedex 9, France, and [⊥]Nanoelectronics Centre, Advanced Technology Institute, University of Surrey, Guildford, GU2 7XH, U.K.

ABSTRACT Aqueous dispersions of functionalized carbon nanotubes (CNTs) are now widely used for biomedical applications. Their stability in different *in vitro* or *in vivo* environments, however, depends on a wide range of parameters, such as pH and salt concentrations of the surrounding medium, and length, aspect ratio, surface charge, and functionalization of the applied CNTs. Although many of these aspects have been investigated separately, no study is available in the literature to date, which examines these parameters simultaneously. Therefore, we have chosen five types of carbon nanotubes, varying in their dimensions and surface properties, for a multidimensional analysis of dispersion stability in salt solutions of differing pH and concentrations. Furthermore, we examine the dispersion stability of oxidized CNTs in biological fluids, such as cellular growth media and human plasma, and their toxicity toward cancer cells. To enhance dispersibility and biocompatibility, the influence of different functionalization schemes is studied. The results of our investigations indicate that both CNT dimensions and surface functionalization have a significant influence on their dispersion and *in vitro* behavior. In particular, factors such as a short aspect ratio, presence of oxidation debris and serum proteins, low salt concentration, and an appropriate pH are shown to improve the dispersion stability. Furthermore, covalent surface functionalization with amine-terminated polyethylene glycol (PEG) is demonstrated to stabilize CNT dispersions in various media and to reduce deleterious effects on cultured cells. These findings provide crucial data for the development of biofunctionalization protocols, for example, for future cancer theranostics, and optimizing the stability of functionalized CNTs in varied biological environments.

KEYWORDS: carbon nanotubes · biomedical applications · dispersion stability · bionanotechnology · surface functionalization · biocompatibility

Since their discovery, the properties and applications of carbon nanotubes (CNTs) have been investigated intensively. While researchers initially focused on their extraordinary physical properties and related applications, research interests have now shifted toward the use of CNTs in the field of biomedicine. When it was discovered in 2004 that carbon nanotubes are able to penetrate cellular membranes, they emerged as a potential new class of intracellular transporters for a number of cargos, such as proteins,[1,2] peptides,[3,4] nucleic acids,[5,6] and drugs.[7−10] At about the same time it was realized that the intrinsic fluorescence properties of carbon nanotubes enable their application as biological imaging agents.[11,12]

For any applications, CNTs usually have to be functionalized in order to render them soluble in water, improve their biocompatibility, and/or allow for the conjugation with further molecules. A widely used type of functionalization is based on the use of surfactants, which attach to or wrap around the tubes in a noncovalent manner. A plethora of molecules has been investigated for this purpose, from conventional, low molecular weight-surfactants[13,14] to (poly-)peptides,[15] proteins,[16] nucleic acids,[17] bile salts,[18] polymers,[19] PEG-composites,[20] and many more. Another popular method for chemical modification of carbon nanotubes (CNTs) is acid oxidation, which has its roots in 1998 when Liu *et al.* discovered that single-walled carbon nanotubes (SWNTs) can be converted from nearly endless, highly tangled ropes into short, open-ended pipes, behaving as individual macromolecules.[21] By introducing carboxylic and other oxygen-containing groups to the otherwise inert carbon nanotube surface,[22] this process has enabled the covalent attachment of functional molecules[23−26] and additionally renders the nanotubes soluble in water. However, it also generates so-called "oxidation debris" by breaking up CNTs during oxidation[27] or oxidizing carbonaceous, nontubular structures present in pristine CNT samples.[28] Oxidation debris has been shown to consist of partially oxidized polyaromatic fragments,[29] which are known to attach to the CNT surface by π-stacking

*Address correspondence to j.mcfadden@surrey.ac.uk.

Received for review January 12, 2010 and accepted March 31, 2010.

Published online April 9, 2010. 10.1021/nn100069k

and increase the stability of CNT dispersions by acting as a surfactant.[30] Though mostly advantageous, this can be a pitfall for effective covalent functionalization of CNTs, if the latter occurs at the level of the debris and not the actual CNT surface. Washing with 0.01 M NaOH upon acid oxidation has been reported to remove oxidation debris by converting the acidic groups of the debris to their conjugate salts, which ultimately leads to the dissolution of debris due to enhanced aqueous solubility.[31,32]

Once carbon nanotubes are functionalized, they are usually readily dispersible in water. However, all physiological fluids, whether cell culture media, interstitial fluids or blood, contain various proteins and other organic molecules, as well as high salt concentrations and sometimes different pH. Hence, it is crucial for CNT formulations with intended use in *in vitro* or *in vivo* environments to be stable under these conditions. It is already known that the solubility of oxidized CNTs depends on the pH and decreases with increasing salt concentration.[33,34] Another important factor is the presence or absence of plasma proteins, which are able to attach to the CNT surface and promote CNT solubilization, but may also replace functional surface coatings. Salvador-Morales *et al.*, for example, have shown that plasma protein binding to CNTs is highly selective and that fibrinogen and apolipoproteins are the proteins binding to CNTs with the greatest avidity.[35] Additionally, they found that CNTs can activate the human complement system and cause immune reactions by binding factor C1q. Hence, efficient and stable surface functionalization is a crucial step toward CNT biocompatibility and stability in biological fluids. CNT dimensions also have become the subject of intense discussions when it was reported by Poland *et al*. that long, rigid multiwalled CNTs can induce asbestos-like pathogenic behavior when introduced into the abdominal cavity of mice, due to frustrated phagocytosis.[36] However, this study was carried out within a framework of occupational health, so the CNTs used were much longer ($>$20 μm) than CNTs applied in biomedical studies ($<$1 μm) and the application route was wholly artificial, as the nanotubes were administered by injection into the peritoneal cavity instead of having been breathed in. The length-dependent effect of short CNTs at the cellular level has been investigated in a study by Becker *et al.*[37] Therein, they demonstrated that human fibroblasts selectively absorb DNA-wrapped single-walled CNTs shorter than about 200 nm, which thereupon induced significant reduction of cell viability when present at high concentrations (between 200 and 400 μg/mL).

Many aspects concerning the dispersion, stability, and the behavior of CNTs in biological settings have already been investigated in separate studies, but not all in a concurrent manner or performed such that immediate comparisons in different ambient systems could be made. This article presents a multidimensional stability analysis of five different types of single-, double-, and multiwalled nanotubes (SWNTs, DWNTs, and MWNTs) as a function of both buffer pH and salt concentration. To examine the influence of oxidation debris, the samples were analyzed before and after removal of the debris. All samples were characterized by atomic force microscopy (AFM), and phase analysis light scattering (PALS) to obtain information on sample morphology and particle size. We then investigated the stability of oxidized SWNT dispersions in cellular growth media with varying serum concentrations, as well as human plasma. Because the dispersion state is a definite factor influencing cell uptake and biodistribution, we have also tested the influence of different functionalization methods (RNA-wrapping or covalent PEGylation) to enhance the dispersibility of oxidized SWNTs in these environments. Finally, the effect of all samples on WiDr colon cancer cells was investigated by means of cell viability assays, and RNA-wrapping and covalent PEGylation are discussed as options to improve CNT biocompatibility.

RESULTS AND DISCUSSION

Functionalization of CNTs and Sample Characterization. Acid oxidation is commonly used to render pristine CNTs soluble in water and introduce functionalities to the tube surface. In this study, the same acid oxidation protocol was applied to all samples. Because different types of CNTs exhibit different susceptibilities toward acid oxidation, varying extents of CNT shortening were observed, as demonstrated by AFM analysis (Figure 1). Nanolab SWNTs and long and thin MWNTs remained most intact, followed by DWNTs, and finally CoMoCAT SWNTs and short and thick MWNTs. In the case of CoMoCAT SWNTs, this is likely due to their smaller diameter (~0.8 nm) in comparison to Nanolab SWNTs (~1.5 nm), which makes them more prone to destruction by acids and sonication.[29] In the case of short and thick MWNTs, however, it seems likely that the reduction in average particle size is due to size fractioning of the CNTs during ultracentrifugation. The pristine tubes exhibit diameters from 110 to 170 nm and hence, oxidation of the outer layer appears to be insufficient to solubilize such heavy tubes. Only the shortest and thinnest CNT species in the sample appear to have been rendered soluble by oxidation, so that they remain in the supernatant during high-speed ultracentrifugation. Indeed, AFM height analysis showed that most tubes in the sample after acid oxidation had diameters between 15 and 40 nm and few up to 80 nm (data not shown). Furthermore, the yield was only 1%, compared to 5 and 15% for the other samples.

Phase analysis light scattering (PALS) measurements of 20 μg/mL oxCNT dispersions in water were carried out to obtain the size distributions of the various samples. The mean values "*l*" of the obtained size

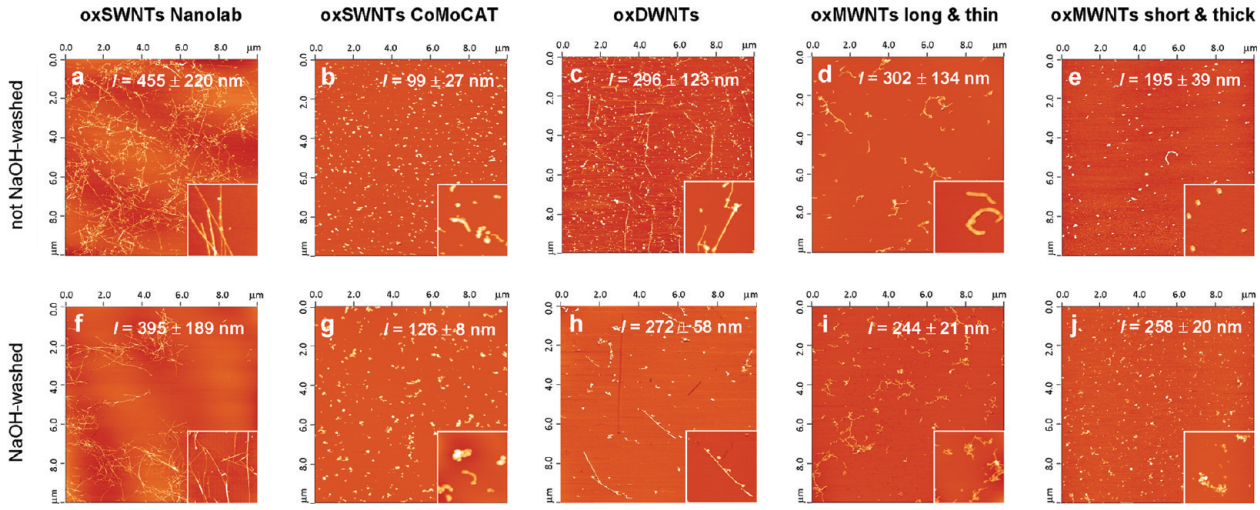

Figure 1. Characterization of the CNT samples by atomic force microscopy (all images 10 μm², insets 0.8−2.5 μm²) and PALS (*l* = transformed mean of CNT length distribution ± full width at half-maximum). Concentrations are between 1 and 10 μg/mL.

distributions were subject to a mathematical transformation to account for the anisotropic shape of CNTs (see Supporting Information for details) and are displayed in each panel of Figure 1. The results are in good agreement with the AFM results, except probably in the case of the Nanolab oxSWNTs, of which the majority seems to be longer than the *l* value suggests. However, this sample also contains very small CNT fragments barely visible in the AFM images, thus lowering the mean length obtained.

The PALS data furthermore indicate that removal of oxidation debris by NaOH washing changes the mean values of the size distributions. In the case of CoMoCAT SWNTs and short and thick MWNTs the mean particle size becomes slightly larger, whereas in the case of the other CNT samples it decreases to some extent. A possible explanation might lie in the effect of oxidation debris on the bundling states of the nanotubes. In the case of longer nanotubes, such as Nanolab SWNTs, DWNTs, and long and thin MWNTs, oxidation debris might promote bundling by gluing nanotubes to each other, as illustrated in Figure 2. Removal of the debris would lead to debundling of the tubes and thus to a decrease of the mean particle size. Short nanotubes, however, are more likely to form well-dispersed, micelle-like structures: In this case, removal of oxidation debris might result in the formation of agglomerates, as observed for CoMoCAT oxSWNTs and short and thick MWNTs in the AFM images (Figure 1g,j), and hence result in an increase of mean particle size.

Another interesting fact is that the full width at half-maximum (fwhm) decreases after NaOH washing, indicating a narrower size distribution. This might again be a reflection of the debundling behavior, as described above. Debundling of long CNTs by NaOH washing removes the largest structures, whereas agglomeration of short CNTs after removal of oxidation debris removes the smallest structures; both resulting in a narrower size distribution.

To further investigate the effect of NaOH washing on the morphology of oxCNTs, Nanolab oxSWNTs were examined by Raman spectroscopy and high-resolution

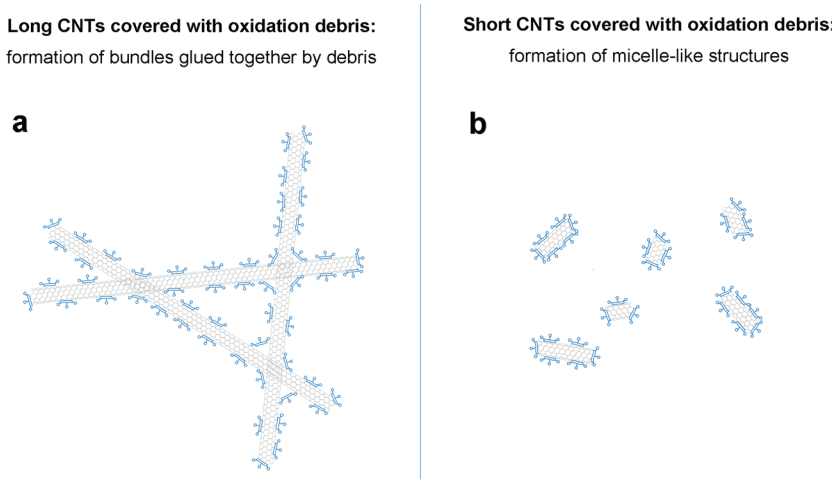

Figure 2. Possible effect of oxidation debris on the bundling behavior of (a) long CNTs, suggesting the formation of bundles, and (b) short CNTs, suggesting the formation of micelle-like structures.

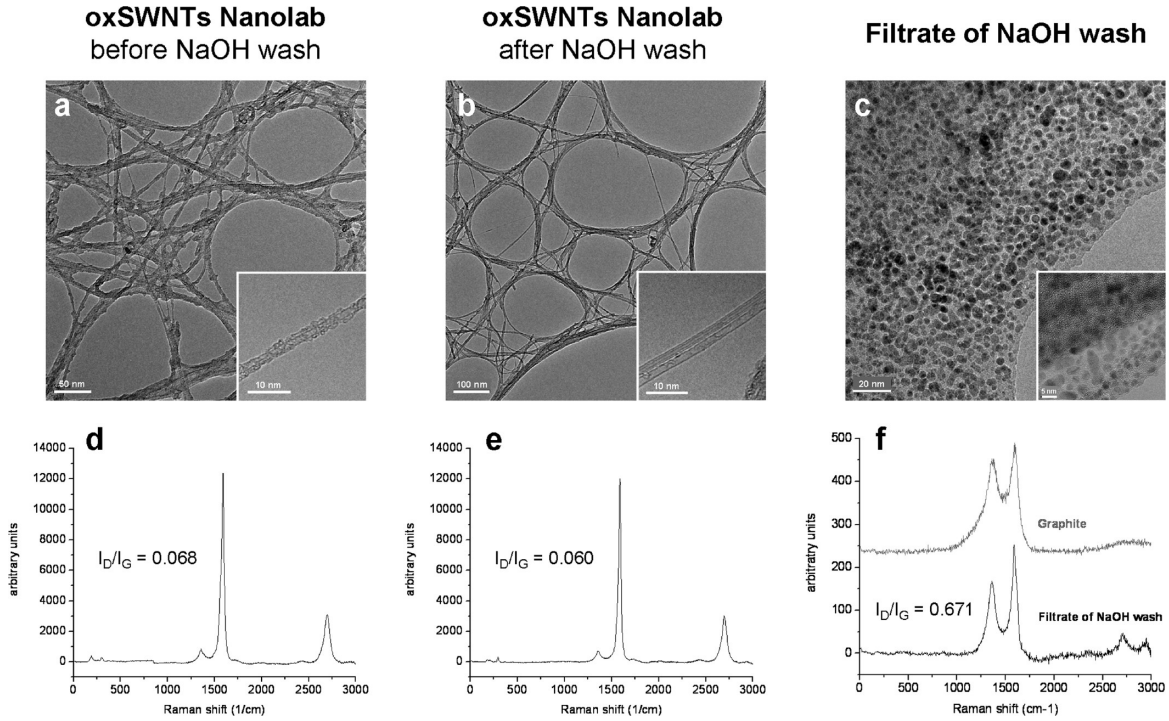

Figure 3. Characterization of oxSWNTs Nanolab before and after NaOH wash, as well as of the oxidation debris in the filtrate of the NaOH wash. (a−c) HRTEM analysis, demonstrating the removal of oxidation debris by NaOH washing and the nontubular composition of the debris. (d−f) Raman analysis of the same sample to compare I_D/I_G ratios and demonstrate the resemblance of the filtrate's Raman spectrum to that of common graphite.

transmission electron microscopy (HRTEM) before and after NaOH washing (Figure 3). In addition, the oxidation debris in the filtrate of the NaOH wash was analyzed by the same methods to obtain an idea of its composition. Figure 3a demonstrates that the surface of the unwashed oxSWNTs is covered with a uniform layer of oxidation debris, whereas the tubes in the washed samples (Figure 3b) feature a cleaner surface (also visible in the AFM images in Figure 1). HRTEM analysis of the debris fraction reveals a nontubular, globular shaped structure (Figure 3c), mainly consisting of carbon, oxygen, and sodium, as detected by energy-dispersive X-ray spectroscopy (EDX) analysis (see Figure S3 in the Supporting Information). It furthermore shows that the sample also contains a fair quantity of double-walled nanotubes (Figure 3b). Raman analysis of the CNTs showed a slight decrease of the I_D/I_G ratio from 0.068 to 0.060 after NaOH washing, indicating the removal of defective material from the sample. Furthermore, a change in the radial breathing modes (RBMs) can be observed (see also Figure S4, Supporting Information). The spectrum of the unwashed sample (Figure 3d) features two main peaks at 188 and 295 cm^{-1}, relating to accumulated diameters at 1.27 and 0.79 nm. In the spectrum of the NaOH-washed sample (Figure 3e), however, the first peak is split up into four intense peaks ranging from 181 to 213 cm^{-1} with much lower intensities. This is indicative of a narrower diameter distribution, that is, due to removal of a defective outer layer of the present double-walled tubes or dissolution of slightly larger diameter tubes. The second peak at 295 cm^{-1}, relating to CNTs with a diameter of about 0.79 nm, remains unchanged. The Raman spectrum of the oxidation debris in the filtrate (Figure 3f) bears a close resemblance to the spectrum of common graphite and indicates that the debris consists of highly disordered graphitic carbon. The lack of RBMs confirms the absence of smaller more ordered tubular structures in the form of SWNTs.

Besides the samples' morphologies, their zeta potentials were measured as a function of pH. The zeta potential is a measure of electrostatic interactions between colloidal particles and has been used in the literature to investigate the density of acidic sites on the surface of MWNTs and the stability of the colloidal MWNT dispersions.[38] An increase in absolute zeta potential leads to enhanced electrostatic repulsion and is hence associated with improvement of the stability of particle dispersions. Herein, short and thick oxMWNTs were chosen for zeta potential measurements, as they contain the largest tubes with the lowest aspect ratio and hence afford the best and most accurate results with the phase analysis light scattering (PALS) technique, which is normally used for spherical colloids. Both unwashed and NaOH-washed oxMWNTs were investigated to account for the effect of oxidation debris. Figure 4 shows that in both cases the zeta potential is least negative at pH 2. It then becomes more negative

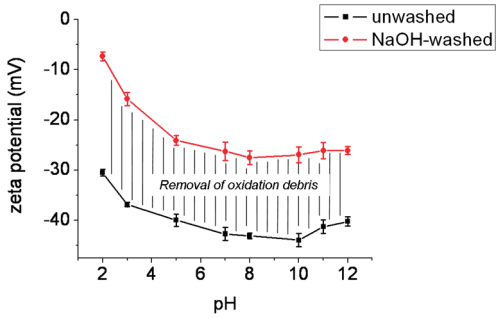

Figure 4. Zeta potential of short and thick MWNTs (unwashed and NaOH-washed) as a function of pH. The zeta potential decreases with increasing pH as more and more carboxylic groups become deprotonated. The zeta potential of the unwashed sample is higher because the oxidation debris contains a major part of the samples' functionalities.

with increasing pH, as more carboxylic groups become deprotonated, and finally stabilizes around pH 8. When comparing the two different samples, it becomes apparent that the zeta potential of the unwashed sample is more negative than that of the NaOH-washed samples over the whole pH-range. This is likely due to the presence of oxidation debris in the unwashed sample, which contains a major part of the samples' functionalities[38,39] and hence contributes to the total zeta potential, as long as it is attached to the CNT surface. At a basic pH, however, the debris detaches from the tubes, and since the size of the particles in the debris is no longer large enough to give rise to light scattering it ceases to contribute to the zeta potential, which also explains the slight increase at a pH above 10.

Stability Studies of oxCNT Dispersions in Buffers of Varying pH and Concentrations. The pH and salt concentration in an aqueous medium highly influences charged molecules and objects within their boundaries. Thus, the stability of CNT dispersions is also influenced by pH and salt concentration of the environment, and if they are to be used for theranostic purposes, these aspects must be studied in detail. Hence, we have conducted a multiparameter study of CNT dispersion stability by subjecting dispersions of five different types of oxidized SWNTs, DWNTs, and MWNTs (with and without oxidation debris) to buffers of varying concentrations and pH (2−12). As discussed previously, oxidation debris tends to stabilize CNT dispersions by acting as a pseudosurfactant or charge buffer. The stability of each sample was then assessed and scored after 4 days according to a scale from 0 to 4, as described in Table 1 and Figure S1 in the Supporting Information. The semiquantitative character of this method has been validated as described in Figure S2 in the Supporting Information.

TABLE 1. Methodology for Scoring the Stability of oxCNT Dispersions in Buffers

score	extent of precipitation	color/shading of supernatant	stability of dispersion (%)
0	total	clear	0−5
1	heavy	light gray	5−10
2	medium, clearly visible	mid gray	10−25
3	little, barely visible	dark gray	25−50
4	no visible agglomerates	dark gray	50−100

The results of the following study will be discussed in the framework of the Derjaguin, Landau, Verwey, and Overbeek (DLVO) theory,[40,41] which describes the stability of colloidal solutions as a function of attractive forces, such as van der Waals and $\pi-\pi$ interactions, and repulsive forces caused by the electrostatic double layer surrounding each particle. Both the zeta potential and width of the electric double layer contribute to the total repulsive force. A higher absolute zeta potential leads to enhanced electrostatic repulsion and is hence a major factor influencing dispersion stability. Another aspect affecting oxCNT dispersion stability is the type of counterions present, giving rise to a so-called "lyotropic effect". Although counterions of the same valence have similar critical agglomeration concentrations (CACs), small differences can exist owing to the different ion sizes. The order of the CAC for monovalent cations is $H^+ > Cs^+ > Rb^+ > NH_4^+ > Na^+ > Li^+$, indicating that Na^+ ions have a greater capability to induce agglomeration in dispersions than H^+ ions. The lyotropic effect is of considerable importance in this experiment because of the manner in which the buffers were prepared (citrate buffers for pH 2−6 and phosphate buffers from pH 7 to 12), leading to the lowest Na^+ concentrations at pH 2 and 7 and highest Na^+ concentrations at pH 6 and 12.

Taken together, the stability of the CNT dispersions is influenced by three main parameters: the zeta potential, the Na^+ concentration of the buffers, and the presence of oxidation debris in unwashed oxCNT samples. This is illustrated in Figure 5, in which both zeta potential (A) and Na^+ concentration (B) were plotted as a function of pH and normalized so that the highest absolute zeta potential and the lowest Na^+ concentration corresponded to a value of 1 (optimal dispersion stability), and the highest Na^+ concentration and lowest absolute zeta potential corresponded to a value of 0 (minimal dispersion stability). In the case of the unwashed sample, a third curve (C) was generated to account for the surfactant properties of oxidation debris in the unwashed sample, which was normalized in the same fashion. The resulting curves R_1 and R_2 are combinations of the three effects; generated in a way to best correlate with the experimental data. In the case of the NaOH-washed samples, both effects A and B were weighed equally. In the case of the unwashed samples, however, the experimental data (Figure 6) suggest that the effect of the oxidation debris (C) is dominating, which was implicated by giving it a higher weight

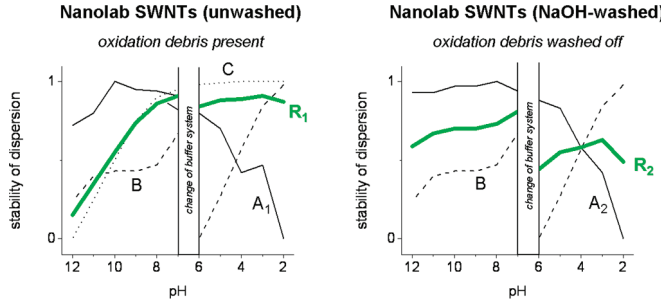

Figure 5. Illustration of the various factors affecting CNT dispersion stability with curve A being the effect of the zeta potential, curve B being the effect of the Na^+ concentration, and curve C being the effect of the oxidation debris' surfactant properties as functions of pH. The resulting green curves R_1 and R_2 are a combination of effects A−C. A *y*-value of 1 corresponds to optimal dispersion stability and a *y*-value of 0 to minimal dispersion stability.

(75%) than the effects A and B, which were each weighted with 12.5%. This semiempirical observation can then be used to capture a semianalytical trend that could be effective in describing the dispersion efficacy of the multidimensional parameters we have used in this study.

Effect of Buffer Concentration. Figure 6 shows the results of our multiparameter stability study, looking at the effects of pH and salt concentration on various types of oxCNT dispersions. With regard to the salt (buffer) concentration, all oxCNT dispersions agglomerate more readily as it increases, regardless of the pH. This effect originates from the compression of the electrical double layer surrounding the oxCNTs by high salt concentrations, which destabilizes dispersions, as also described by Peng *et al.*[33]

Effect of CNT Type and Shape. The experiment further shows that the dimensions of the CNTs after oxidation clearly influence the stability of the resulting CNT dispersions. Sorting the different CNT samples by length according to the AFM and PALS data leads to the following order: oxSWNTs Nanolab ≫ oxDWNTs ≫ oxMWNTs (long and thin) ≫ oxMWNTs (short and thick) ≫ oxSWNTs CoMoCAT. A comparison with the solubility profiles in Figure 6 indicates that the order is the same for dispersion stability: oxSWNTs Nanolab being most sensitive to changes in buffer pH and concentration and CoMoCAT oxSWNTs and short and thick MWNTs being somewhat insensitive to these parameters. This behavior can be attributed to the fact that long CNTs are prone to increased intertube attraction due to van der Waals forces and $\pi-\pi$ interactions (assuming a similar extent of surface oxidation) and are thereby more likely to form agglomerates and bundles in comparison to short CNTs.

Effect of pH. The effect of pH is in fact a superposition of three separate factors—zeta potential, Na^+ ion concentration, and presence of oxidation debris. To simplify discussion of the experimental findings, we combined these effects in a resulting curve, as illustrated in Figure 5. Curve A illustrates the effect of the zeta potential on dispersion stability: In the case of carbon nanotubes, the absolute zeta potential is lowest at low pH, where most carboxylic groups are protonated (and hence uncharged), resulting in poor aqueous solubility. Theoretically, the lowest solubility would appear around the isoelectric point of CNTs or "point of zero charge", which lies at a pH of about 1.[42] The further the pH deviates from the isoelectric point, the more carboxylic groups become deprotonated, leading to a higher absolute zeta potential and enhanced dispersion stability.[43] Curve B describes the lyotropic effect caused by changes in the Na^+ concentration, due to the way the buffers are composed (the curve was generated by inverting and normalizing the Na^+ concentration in the buffers). It features two minima at pH 6 and 12, where the Na^+ concentration is highest and thus exerts the strongest destabilizing effect. Curve C was generated to account for the effect of oxidation debris in the unwashed sample. Its interaction with the CNT surface is strongest at low pH and becomes weaker with increasing pH, until it completely detaches at a pH > 11 due to increased hydrophilicity of both the debris and the CNTs,

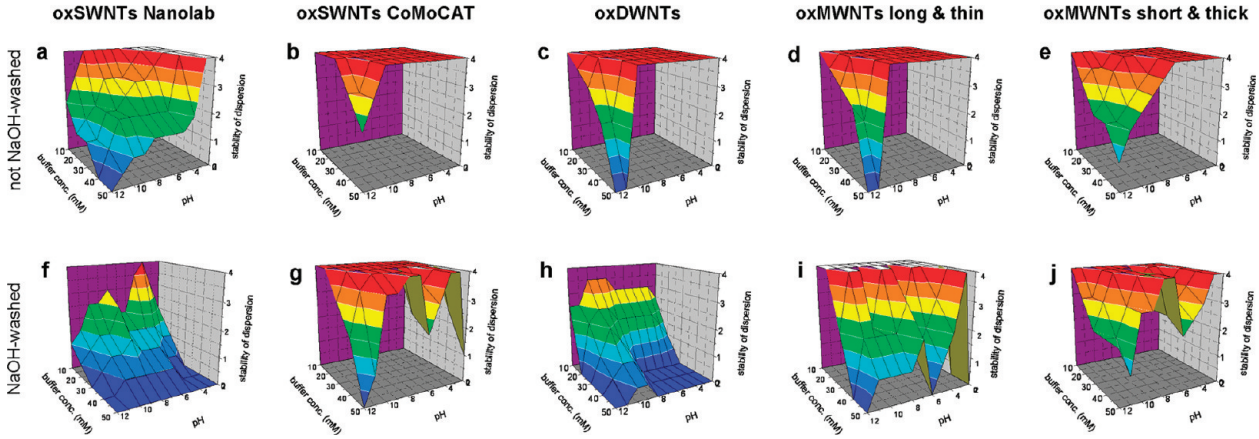

Figure 6. Results of the stability studies of oxCNTs at a pH range from 2 to 12 and buffer concentrations ranging from 10 to 50 mM. Red coloring corresponds to optimal dispersion stability and blue coloring corresponds to minimal dispersion stability.

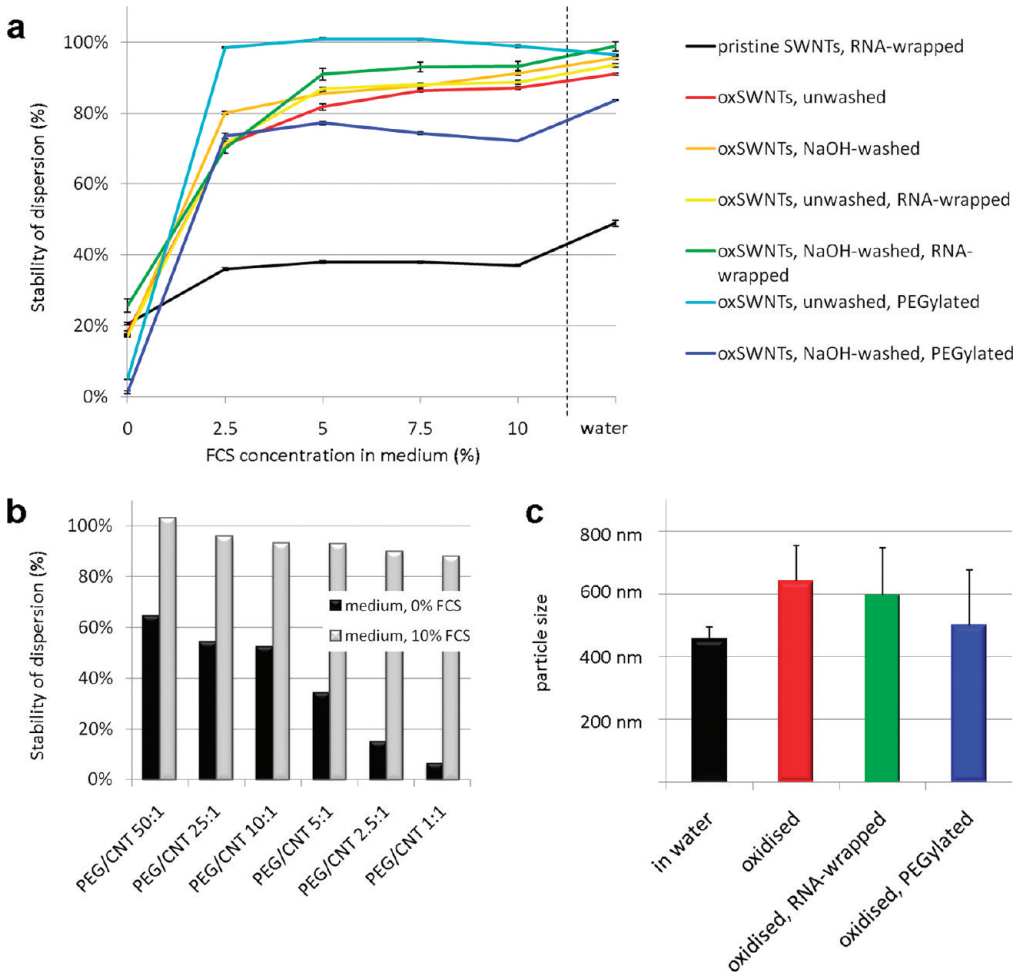

Figure 7. (a) Stability of oxidized SWNTs (unwashed & NaOH-washed) with different surface coatings in cellular growth medium of varying serum concentrations (0−10%). Note that the error bars are included, but very small and thus hardly visible. (b) Influence of the PEG density on the stability of oxidized SWNTs in cellular growth medium. (c) Stability of oxidized SWNTs with different surface coatings in human plasma.

which weakens the $\pi-\pi$ interactions. In fact, Figure 6 shows that unwashed CNTs are much less susceptible to agglomeration at lower buffer concentrations than their NaOH-washed counterparts. Only at pH $>$ 11, where total detachment of the debris occurs, does the solubility of unwashed oxCNTs drop almost instantly. Because the experimental results indicate that the shape of the stability profiles is dominated by this effect, it was given a higher weighting in the semiempirical model than the effect of zeta potential and Na^+ concentration, as indicated above.

In summary, CNT dispersions containing short and unwashed tubes exhibit the best stability. However, the presence of oxidation debris is not always desirable, especially if molecules are to be attached to the CNT surface in a covalent manner. In these cases, agglomeration can be evaded by using buffers of low concentrations and low Na^+ content.

Stability Study of SWNTs in Cellular Growth Media of Varying Serum Concentrations. For biomedical use, the requirements of CNTs to be stable in both buffer solutions and the various physiological environments they encounter in the body are critical prerequisites. The stability of oxidized Nanolab SWNTs with different surface functionalizations was therefore investigated in cellular growth media of varying serum concentrations, as well as in human plasma (Figure 7). The two selected functionalization schemes, PEGylation and RNA-wrapping, are of particular clinical importance. PEGylation of drugs and nanoparticulate-drug formulations is a widely used approach to reduce immunogenicity and nonspecific interactions with proteins, as well as to enhance blood circulation times. RNA-wrapping, on the other hand, is highly relevant with regard to the delivery of therapeutic RNA, such as siRNA and mRNA, which are nucleic acids directly functional in cells. Furthermore, RNA is less mutagenic than DNA, as it cannot integrate into the host chromosome and can be efficiently used for the purification of carbon nanotubes, if the RNA is subsequently removed by the enzyme RNase, as demonstrated in previous work of our group.[17]

We tested the dispersion stability of various oxidized SWNT samples in cell medium by incubating them in the medium for 24 h, followed by a centrifugation step to remove agglomerates that might have formed. The amount of remaining nanotubes in the supernatant was determined by UV−vis absorption spectroscopy with a SWNT in water dispersion serving as the 100% value. To examine the influence of the serum concentration, five different serum concentrations were tested, ranging from 0 to 10%. Furthermore, we compared unwashed and NaOH-washed SWNTs and investigated whether RNA-wrapping and PEGylation can improve dispersion stability. Figure 7a shows that all investigated CNT formulations were poorly stable in serum-free cellular growth medium. This is not surprising, since serum-free medium is nothing more than a solution of various salts and other compounds at a concentration of 154 mM—a concentration, at which all oxCNT formulations investigated in this study immediately precipitated. However, the presence of only 2.5% fetal calf serum (FCS) increased the dispersion stability by more than 50%, presumably due to serum proteins attaching to the CNT surface. A further increase in FCS concentration resulted in 80−90% stability and thus became comparable to that of CNTs in water. The highest stability was obtained for unwashed, PEGylated oxSWNTs with a stability of 100% in both water and FCS-supplemented cell medium, whereas RNA-wrapped, nonoxidized CNTs were the least stable with only 49% in water and 38% in FCS-supplemented cell medium. The other oxidized CNTs gave similar high levels of stability with PEGylated, NaOH-washed oxSWNTs being the least stable. In this particular case, the nanotubes precipitated during the PEGylation reaction and although they could be redispersed after completion of the coupling reaction, the sample nevertheless seemed to have forfeited stability.

In a separate study we tested whether the PEG density affects the dispersion stability of PEGylated oxSWNTs in cell medium. Instead of Nanolab SWNTs we have used oxidized CoMoCAT SWNTs for this experiment, as they are more stable and thus also allowed us to study the dispersion stability in serum-free cell medium, which, in comparison, caused almost complete precipitation of PEGylated Nanolab oxSWNTs. The oxidized nanotubes were conjugated to amine-terminated PEG molecules at initial weight ratios ranging from 50:1 to 1:1 (50:1 was the ratio used in the experiment presented in Figure 7a). Unreacted PEG was removed after the reaction. Figure 7b shows that higher PEG densities indeed improve the dispersion stability in serum-free cell medium to a significant extent. An initial PEG/CNT ratio of 50:1 is able to keep 60% of the nanotubes in dispersion, likely due to electrostatic repulsion of the positively charged PEG chains. At lower PEG/CNT ratios, this effect decreases until it is no longer sufficient to maintain the systems' dispersion stability. A similar trend is observed in cell medium containing 10% FCS, again with the highest initial PEG/CNT ratio affording the highest dispersion stability. It is, however, much less substantial, which is in accordance with the fact that PEG prevents nonspecific interactions with serum proteins (seen also in Figure 7c). The observed stabilizing effect caused by serum proteins is likely due to electrostatic interactions of the proteins with the terminal amine group of the PEG chains, resulting in steric stabilization, rather than to proteins adsorbing onto the CNT surface.

We have also tested the dispersion stability of the SWNT samples in human plasma in order to simulate the therapeutic application of CNTs. In this case UV−vis absorption spectroscopy cannot be used, as plasma absorbs at wavelengths around 600−1000 nm. Instead, we measured the increase in particle size due to agglomeration effects by PALS measurements after a 96 h incubation period in plasma. The particle size of the same sample in water served as a control. Figure 7c shows that after the incubation period, the mean particle size increased from 455 (oxCNTs in water) to 642 nm, which is likely due to attachment of plasma proteins, such as fibrinogen, albumin, and apolipoproteins, to the CNT surface.[35] Note that fibrinogen is only present in plasma, but not in serum. These nonspecific interactions between plasma proteins and CNTs can be prevented by an appropriate surface functionalization scheme. In this article, we have tested RNA-wrapping and covalent PEGylation as two possibilities. As Figure 7b shows, RNA-wrapping resulted only in a slight decrease of mean particle size (about 30 nm), which is likely due to degradation of RNA in biological environments by RNases after a certain period. Covalent PEGylation, however, decreased the mean particle size by 140 nm (from 642 to 502 nm), which is only 46 nm more than the mean particle size of the oxCNT sample in water. This shows that covalent PEGylation can effectively prevent nonspecific adsorption of plasma proteins to the nanotube surface.

These experiments demonstrate that the dispersion properties of oxCNTs are significantly changed when passing from a chemical environment to a biological environment due to high salt concentrations and the attachment of plasma/serum proteins to the CNT surface. Although the latter can help to stabilize oxCNT dispersions, especially at high salt concentrations as found in the body, it might be disadvantageous when it replaces functional surface coatings. Thus, it is usually the best option to design carbon nanotubes with intended biomedical use in such a way that nonspecific interactions with proteins are prevented, for example by PEGylation.

Cell Viability Assays. A study by Becker *et al.*[37] demonstrated that adherent human lung fibroblasts preferentially take up nanotubes shorter than 200 nm, indicating

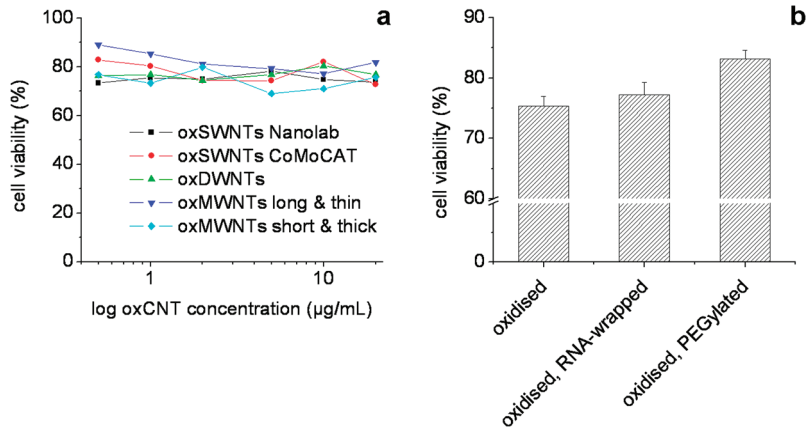

Figure 8. Results of adapted MTT cytotoxicity assay on WiDr human colon cancer cells after an incubation period of 96 h with various samples of oxCNTs (NaOH-washed) at concentrations ranging from 0.5 to 20 μg/mL. (a) Dose−response curves for the five different types of CNTs, showing no dose-dependent cytotoxicity at this concentration range, (b) average cell viability for Nanolab oxSWNTs with different surface functionalizations, indicating that PEGylation results in a statistically significant enhancement in cell viability. The "cells only" control correlates with 100% cell viability.

that the dispersion state of CNTs is likely to influence cellular exposure, cytotoxicity, and response of cells to CNTs. They observed acute cytotoxicity only for very high CNT concentrations (197 and 360 μg/mL), which is about 10-times higher than concentrations typically used in *in vitro* and *in vivo* experiments. However, their study examined only one CNT sample (CoMoCAT SWNTs wrapped with DNA), which was separated into different length fractions. In our experiments, we incubated WiDr colon cancer cells with five different oxCNT samples (all NaOH-washed) at various concentrations for 96 h to investigate the effect of CNT size and dispersion properties on cell viability. The applied MTT viability assay is a standard colorimetric assay, which measures the activity of mitochondrial enzymes reducing the MTT reagent (thiazolyl blue tetrazolium bromide) to yield a purple formazan product.[44] Because it has been reported that some viability assays, including MTT, can lead to false positive results when used with CNTs due to assay reagent adsorbing to the CNT surface,[45] we exchanged the cell medium containing the CNT with fresh medium just before adding the MTT dye. Our main goal was to examine the effect of CNT dimensions and different surface funtionalizations on cell viability at concentrations commonly used for *in vitro* and *in vivo* experiments.

Figure 8 shows the viability curves of WiDr colon cancer cells as measured by an adapted MTT assay, which have been incubated with the five different oxCNT samples for 96 h. The viability curves do not show a dose-dependent toxicity, which might be attributed to the fact that cellular uptake of CNTs is incomplete, and thus the effective CNT concentrations acting upon the cells are lower than the inoculation concentrations. All CNT samples, however, induced about 5−15% cell death after the incubation period, independent of the inoculation concentration. This might be due to inhibition of cell proliferation[46] or decreased adhesion,[47] which are both effects that would be predominantly observed for long incubation times, as seen in our study. A length-dependent effect on cell viability was not observed for the tested concentration range, but might become apparent at higher CNT concentrations. In the second part of this study, the effect of two different types of surface functionalizations on cell viability was examined. RNA-wrapping did not significantly reduce the cytotoxic effect of the CNT samples, but PEGylation resulted in a statistically significant enhancement in cell viability (83% compared to 75%). This might be due to better dispersion stability or could be a consequence of the ability of PEGylation to reduce nonspecific uptake by cells,[48] an ability, which is often utilized in the framework of targeted drug delivery studies.

In parallel studies, we are currently looking at more subtle changes in cellular behavior after CNT exposure, such as stress response. This also includes a greater number of cell lines, as previous studies have demonstrated that most toxicological effects of CNTs depend on the cell type. The results of these studies will be published separately in the near future.

CONCLUSIONS

This study is the first of its kind to present a multiparameter stability analysis of various types of functionalized CNTs in environments relevant for biomedical studies. Its findings are of considerable value for selecting the most appropriate material and functionalization protocol for *in vitro* or *in vivo* applications. We demonstrate that the same acid oxidation protocol leaves some CNT samples nearly unaltered, whereas others are significantly broken up, leading to altered CNT dimensions and surface properties, which in turn influence their dispersion in salt solutions, cellular growth media, and human plasma. A similar diversity was found for the effect of the removal of oxidation debris, which

leaves the tubes with a clean surface, but also impairs dispersion stability. However, functionalization of CNTs with appropriate biomolecules allows for tailoring of their surface properties and is shown to improve dispersion stability, as well as to reduce cytotoxicity. Overall, this study demonstrates that an extended knowledge of CNT dispersion is of paramount importance, if they are to fulfill their promise for applications in the biomedical field, for example as theranostic vehicles. It thereby provides a valuable platform for the development of CNT formulations for current and future biomedical applications.

EXPERIMENTAL SECTION

Material. SWeNT SG 65 were obtained from SouthWest Nano-Technologies *via* Sigma-Aldrich (produced by CoMoCAT, tube diameter 0.8 ± 0.1 nm, carbon content >90% by weight, >50% of tubes are (6,5) chirality, >90% of tubes are semiconducting, order no. 70414, lot no. MKBB63098). SWNTs D1.5L1-5-S were purchased from NanoLab, Inc. (produced by CVD using iron (ferrocene) as catalyst, purity >95%, diameter ~1.5 nm, length 1−5 μm, lot no. 90907). MWNTs 1 and 2 were both obtained from Sigma-Aldrich (MWNTs 1: produced by CVD, outer diameter 10−20 nm, inner diameter 5−10 nm, length 0.5−200 μm, carbon content >95%, order no. 636525, lot no. 03826TB. MWNTs 2: diameter 110−170 nm, length 5−9 μm, carbon content >90%, order no. 659258, lot no. 04121HD). DWNTs were synthesized at CIRIMAT-LCMIE, Université Paul Sabatier in Toulouse, France.

The different nanotube samples are referred to as follows: SWeNT SG 65 as "CoMoCAT SWNTs", SWNTs D1.5L1-5-S as "Nanolab SWNTs", MWNTs 1 as "long and thin MWNTs", MWNTs 2 as "short and thick MWNTs", DWNTs as "DWNTs".

Other chemicals were purchased from Sigma-Aldrich (Poole, U.K.) and used without further treatment. The applied RNA (R6750) was derived from baker's yeast (S. cerevisiae).

Functionalization of CNTs. Acid oxidation of CNTs was carried out as follows: 100 mg of CNTs were dispersed in 20 mL of concentrated nitric acid, sonicated with a tip sonicator (MSE Soniprep 150, amplitude 8 μm) for 6 × 10 s, and incubated in a water bath at 95 °C for 2 h. After oxidation, the acid was diluted with water, and the mixture was centrifuged for 10 min at 50000*g*, followed by extensive washing with water. These pretreated CNTs were then redispersed in a 3:1 mixture of concentrated nitric and sulfuric acid and the above-described process was repeated. Afterward, the oxidized CNTs were vacuum filtered using a 0.2 μm polycarbonate filter (Whatman Ltd.) until the eluate was clear and of neutral pH (unwashed sample). The product was split into two parts, of which one was washed with 0.01 M sodium hydroxide to remove oxidation debris, followed by washing with water until the eluate was clear and of neutral pH (NaOH-washed sample). The filtrate was collected for further analysis. Both parts were then sonicated with a tip sonicator for 6 × 10 s and centrifuged three times at 75000*g* to remove big agglomerates and CNT bundles. The concentration of these dispersions was determined gravimetrically.

To prepare pristine, RNA-wrapped CNTs, 20 mg of RNA was dissolved in 10 mL of water and mixed with 20 mg of pristine CNTs. The mixture was sonicated with a tip sonicator for 6 × 10 s and in a water bath for 90 min. To remove insufficiently functionalized CNTs, the dispersion was centrifuged at 75000*g* for 15 min. The supernatant was collected and filtered through a 0.2 μm polycarbonate filter to remove excess RNA. Finally, the concentration was determined gravimetrically and adjusted to 50 μg/mL or 200 μg/mL. To wrap oxidized CNTs with RNA, 1 mg of RNA was dissolved in 1 mL of water and added to 20 mL of a 50 μg/mL oxCNT dispersion. The mixture was tip sonicated for 6 × 10 s and repeatedly filtered through a polycarbonate filter (0.2 μm pore size) to remove excess RNA. Finally, the functionalized oxCNTs were resuspended in water.

For covalent PEGylation of oxidized carbon nanotubes, an oxCNT dispersion in 1 mM sodium phosphate buffer pH 8.0 was mixed with EDC (2 mM) and sulfo-NHS (5 mM) and stirred at room temperature for 15 min. Next, 0.5 mL of amine-terminated PEG 2000 (50 mM) was added to the mixture, tip sonicated for 10 s, and incubated for 2 h at room temperature while stirring. Finally, the PEGylated oxCNTs were filtered using a 0.2 μm polycarbonate filter, washed abundantly with water to remove excess reagents, and resuspended in water at a concentration of 50 μg/mL.

Sample Characterization. The CNT samples in this work were characterized by atomic force microscopy (AFM), high resolution transmission electron microscopy (HR-TEM), Raman spectroscopy, and zeta potential measurements. For AFM sample preparation, oxCNTs were diluted with water to obtain a concentration of 10 μg/mL and a droplet of 2 μL was placed onto a freshly cleaved mica substrate (1 cm^2) and dried in air. AFM measurements were performed using a PicoPlus instrument (Agilent Technologies, Chandler, AZ) operated in contact mode at room temperature with a lateral scan rate of 1−1.5 Hz at 512 lines. Data analysis was carried out using "Gwyddion 2.9′′, a free SPM data visualization and imaging tool released under the GNU General Public License. HR-TEM and EDX analysis was carried out using a high resolution transmission electron microscope JEOL-EM 2100. Raman spectroscopy measurements were performed using a NT-MDT NTEGRA Spectra Probe NanoLaboratory at an excitation wavelength of 633 nm. The particle size distributions of oxCNT dispersions were measured for 20 μg/mL oxCNT dispersions in water using a Brookhaven ZetaPALS (Holsville, New York) by means of phase analysis light scattering (PALS), and the results were subjected to a mathematical transformation in order to account for the anisotropy of a tubular sample as developed by Cherkasova *et al.*[49] (Supporting Information). The zeta potential ζ was measured using the same instrument and 5 mM citrate or phosphate buffers from pH 2 to 12 (ionic strength = 30 mM), and the results were plotted as a function of pH. Each data point is the mean value of 10 runs, each comprising 20 measurement cycles. The ζ values are calculated from the particle mobilities by means of the Helmholtz−Smoluchowski equation.

Stability Studies of oxCNT Dispersions in Buffers of Varying pH and Concentrations. Solutions of buffer (100 mM) of pH 2 to 12 were produced using mixtures of 100 mM citric acid/trisodium citrate solutions for pH 2−6 and 100 mM monobasic/tribasic sodium phosphate solutions for pH 7−12. As citrate and phosphate have the same valency, this guarantees the same ionic strength for all buffer solutions. Furthermore, the distribution of the pK_a values guarantees good buffering properties over the whole pH range with an exception of pH 9 and 10 (located within the steep part of the titration curve). For these cases, it was separately confirmed that the buffering capacity is sufficient to maintain a stable pH after the addition of oxidized CNTs. In the next step, 20 μg/mL oxCNT solutions were mixed with the buffers at various concentrations to achieve a final oxCNT concentration of 10 μg/mL and final buffer concentrations of 10, 20, 30, 40, or 50 mM. The stability of each solution was rated after 4 days according to a scale from 0 to 4, as described in Table 1 and Figure S1 in the Supporting Information. For more information on method validation please refer to the Supporting Information.

Stability Study of SWNTs in Cellular Growth Medium of Varying Serum Concentration. Fetal calf serum (FCS) was added to MEM-based, phenol red-free cellular growth medium (GIBCO, Invitrogen, Paisley, U.K.) supplemented with GlutaMAX and antibiotics in order to create FCS concentrations of 0%, 2.5%, 5%, 7.5%, and 10%. Next, five different Nanolab SWNT samples were mixed with the different media formulations at final CNT concentrations of 10 μg/mL. The samples comprised pristine, RNA-wrapped SWNTs, oxidized SWNTs (NaOH-washed and unwashed), RNA-wrapped, oxidized SWNTs (NaOH-washed and unwashed), as well as PEGylated, oxidized SWNTs (NaOH-washed and unwashed). After

one day of incubation, all samples were centrifuged at 14500*g* for 10 min, and the supernatants were analyzed by UV−vis spectroscopy at a wavelength of 730 nm, which is outside of the absorption window of FCS.

Evaluating the Effect of the Various Nanotube Preparations on Cell Viability. WiDr cells were cultured in Eagle's minimal essential medium (MEM) supplemented with 2 mM L-glutamine, 10% fetal bovine serum, 1 mM sodium pyruvate, 0.1 mM nonessential amino acids, and penicillin/streptomycin (100 units/mL penicillin and 100 μg/mL streptomycin) for use in a 5% CO_2 in air atmosphere. Cultured cells in single cell suspension were seeded at a density of 10^4 cells per well and incubated for 24 h. The following day, dilution series of all CNT samples in cellular growth media were prepared, and the appropriate amounts of CNTs were added to the wells to obtain final CNT concentrations of 20, 10, 5, 2, 1, and 0.5 μg/mL. After an incubation period of 96 h, the old culture medium containing the CNTs was replaced with fresh medium, and cell viability was evaluated by means of the MTT assay.[44] Each sample was tested in quadruplicate.

Acknowledgment. This work has been performed in the framework of the FP6Marie Curie Research Training Network "CARBIO" (RTN-CT-2006-035616) funded by the European Union. Special thanks to T. Lutz for helpful discussions and advice.

Supporting Information Available: Mathematical transformation for phase-analysis light-scattering results, rating of oxCNT dispersion stability and method validation, EDX analysis of oxidation debris, RBM analysis of Raman data. This material is free of charge *via* the Internet at http://pubs.acs.org.

REFERENCES AND NOTES

1. Kam, N. W. S.; Jessop, T. C.; Wender, P. A.; Dai, H. J. Nanotube Molecular Transporters: Internalization of Carbon Nanotube−Protein Conjugates into Mammalian Cells. *J. Am. Chem. Soc.* **2004**, *126*, 6850–6851.
2. Kam, N. W. S.; Dai, H. J. Carbon Nanotubes as Intracellular Protein Transporters: Generality and Biological Functionality. *J. Am. Chem. Soc.* **2005**, *127*, 6021–6026.
3. Panhuis, M. I. H. Vaccine Delivery by Carbon Nanotubes. *Chem. Biol.* **2003**, *10*, 897–898.
4. Pantarotto, D.; Briand, J. P.; Prato, M.; Bianco, A. Translocation of Bioactive Peptides across Cell Membranes by Carbon Nanotubes. *Chem. Commun.* **2004**, 16–17.
5. Kam, N. W. S.; Liu, Z.; Dai, H. J. Functionalization of Carbon Nanotubes *via* Cleavable Disulfide Bonds for Efficient Intracellular Delivery of SIRNA and Potent Gene Silencing. *J. Am. Chem. Soc.* **2005**, *127*, 12492–12493.
6. Ahmed, M.; Jiang, X. Z.; Deng, Z. C.; Narain, R. Cationic Glyco-Functionalized Single-Walled Carbon Nanotubes as Efficient Gene Delivery Vehicles. *Bioconjugate Chem.* **2009**, *20*, 2017–2022.
7. Liu, Z.; Chen, K.; Davis, C.; Sherlock, S.; Cao, Q. Z.; Chen, X. Y.; Dai, H. J. Drug Delivery with Carbon Nanotubes for *in Vivo* Cancer Treatment. *Cancer Res.* **2008**, *68*, 6652–6660.
8. Bhirde, A. A.; Patel, V.; Gavard, J.; Zhang, G. F.; Sousa, A. A.; Masedunskas, A.; Leapman, R. D.; Weigert, R.; Gutkind, J. S.; Rusling, J. F. Targeted Killing of Cancer Cells *in Vivo* and *in Vitro* with EGF-Directed Carbon Nanotube-Based Drug Delivery. *ACS Nano* **2009**, *3*, 307–316.
9. Heister, E.; Neves, V.; Tîlmaciu, C.; Lipert, K.; Sanz Beltrán, V.; Coley, H.; Ravi, S. R. P.; McFadden, J. Triple Functionalisation of Single-Walled Carbon Nanotubes with Doxorubicin, a Monoclonal Antibody, and a Fluorescent Marker for Targeted Cancer Therapy. *Carbon* **2009**, *47*, 2152–2160.
10. Wu, W.; Li, R.; Bian, X.; Zhu, Z.; Ding, D.; Li, X.; Jia, Z.; Jiang, X.; Hu, Y. Covalently Combining Carbon Nanotubes with Anticancer Agent: Preparation and Antitumor Activity. *ACS Nano* **2009**, *3*, 2740–2750.
11. Liu, Z. A.; Li, X. L.; Tabakman, S. M.; Jiang, K. L.; Fan, S. S.; Dai, H. J. Multiplexed Multicolor Raman Imaging of Live Cells with Isotopically Modified Single Walled Carbon Nanotubes. *J. Am. Chem. Soc.* **2008**, *130*, 13540–13541.
12. Heller, D. A.; Baik, S.; Eurell, T. E.; Strano, M. S. Single-Walled Carbon Nanotube Spectroscopy in Live Cells: Towards Long-Term Labels and Optical Sensors. *Adv. Mater.* **2005**, *17*, 2793–2399.
13. Islam, M. F.; Rojas, E.; Bergey, D. M.; Johnson, A. T.; Yodh, A. G. High Weight Fraction Surfactant Solubilization of Single-Wall Carbon Nanotubes in Water. *Nano Lett.* **2003**, *3*, 269–273.
14. Simmons, T. J.; Bult, J.; Hashim, D. P.; Linhardt, R. J.; Ajayan, P. M. Noncovalent Functionalization as an Alternative to Oxidative Acid Treatment of Single Wall Carbon Nanotubes with Applications for Polymer Composites. *ACS Nano* **2009**, *3*, 865–870.
15. Zorbas, V.; Ortiz-Acevedo, A.; Dalton, A. B.; Yoshida, M. M.; Dieckmann, G. R.; Draper, R. K.; Baughman, R. H.; Jose-Yacaman, M.; Musselman, I. H. Preparation and Characterization of Individual Peptide-Wrapped Single-Walled Carbon Nanotubes. *J. Am. Chem. Soc.* **2004**, *126*, 7222–7227.
16. Lin, Y.; Allard, L. F.; Sun, Y. P. Protein-Affinity of Single-Walled Carbon Nanotubes in Water. *J. Phys. Chem. B* **2004**, *108*, 3760–3764.
17. Jeynes, J. C. G.; Mendoza, E.; Chow, D. C. S.; Watts, P. C. R.; McFadden, J.; Silva, S. R. P. Generation of Chemically Unmodified Pure Single-Walled Carbon Nanotubes by Solubilizing with RNA and Treatment with Ribonuclease A. *Adv. Mater.* **2006**, *18*, 1598–1602.
18. Wenseleers, W.; Vlasov, I. I.; Goovaerts, E.; Obraztsova, E. D.; Lobach, A. S.; Bouwen, A. Efficient Isolation and Solubilization of Pristine Single-Walled Nanotubes in Bile Salt Micelles. *Adv. Funct. Mater.* **2004**, *14*, 1105–1112.
19. O'Connell, M. J.; Boul, P.; Ericson, L. M.; Huffman, C.; Wang, Y. H.; Haroz, E.; Kuper, C.; Tour, J.; Ausman, K. D.; Smalley, R. E. Reversible Water-Solubilization of Single-Walled Carbon Nanotubes by Polymer Wrapping. *Chem. Phys. Lett.* **2001**, *342*, 265–271.
20. Prencipe, G.; Tabakman, S. M.; Welsher, K.; Liu, Z.; Goodwin, A. P.; Zhang, L.; Henry, J.; Dai, H. J. PEG-Branched Polymer for Functionalization of Nanomaterials with Ultralong Blood Circulation. *J. Am. Chem. Soc.* **2009**, *131*, 4783–4787.
21. Liu, J.; Rinzler, A. G.; Dai, H. J.; Hafner, J. H.; Bradley, R. K.; Boul, P. J.; Lu, A.; Iverson, T.; Shelimov, K.; Huffman, C. B.; *et al.* Fullerene Pipes. *Science* **1998**, *280*, 1253–1256.
22. Zhang, J.; Zou, H. L.; Qing, Q.; Yang, Y. L.; Li, Q. W.; Liu, Z. F.; Guo, X. Y.; Du, Z. L. Effect of Chemical Oxidation on the Structure of Single-Walled Carbon Nanotubes. *J. Phys. Chem. B* **2003**, *107*, 3712–3718.
23. Dwyer, C.; Guthold, M.; Falvo, M.; Washburn, S.; Superfine, R.; Erie, D. DNA-Functionalized Single-Walled Carbon Nanotubes. *Nanotechnology* **2002**, *13*, 601–604.
24. Georgakilas, V.; Kordatos, K.; Prato, M.; Guldi, D. M.; Holzinger, M.; Hirsch, A. Organic Functionalization of Carbon Nanotubes. *J. Am. Chem. Soc.* **2002**, *124*, 760–761.
25. Huang, W. J.; Taylor, S.; Fu, K. F.; Lin, Y.; Zhang, D. H.; Hanks, T. W.; Rao, A. M.; Sun, Y. P. Attaching Proteins to Carbon Nanotubes *via* Diimide-Activated Amidation. *Nano Lett.* **2002**, *2*, 311–314.
26. Huang, W. J.; Fernando, S.; Allard, L. F.; Sun, Y. P. Solubilization of Single-Walled Carbon Nanotubes with Diamine-Terminated Oligomeric Poly(Ethylene Glycol) in Different Functionalization Reactions. *Nano Lett.* **2003**, *3*, 565–568.
27. Hu, H.; Zhao, B.; Itkis, M. E.; Haddon, R. C. Nitric Acid Purification of Single-Walled Carbon Nanotubes. *J. Phys. Chem. B* **2003**, *107*, 13838–13842.
28. Shao, L.; Tobias, G.; Salzmann, C. G.; Ballesteros, B.; Hong, S. Y.; Crossley, A.; Davis, B. G.; Green, M. L. H. Removal of Amorphous Carbon for the Efficient Sidewall Functionalisation of Single-Walled Carbon Nanotubes. *Chem. Commun.* **2007**, 5090–5092.
29. Nagasawa, S.; Yudasaka, M.; Hirahara, K.; Ichihashi, T.; Iijima, S. Effect of Oxidation on Single-Wall Carbon Nanotubes. *Chem. Phys. Lett.* **2000**, *328*, 374–380.

30. Rosca, I. D.; Watari, F.; Uo, M.; Akaska, T. Oxidation of Multiwalled Carbon Nanotubes by Nitric Acid. *Carbon* **2005**, *43*, 3124–3131.
31. Verdejo, R.; Lamoriniere, S.; Cottam, B.; Bismarck, A.; Shaffer, M. Removal of Oxidation Debris from Multi-Walled Carbon Nanotubes. *Chem. Commun.* **2007**, 513–515.
32. Fogden, S.; Verdejo, R.; Cottam, B.; Shaffer, M. Purification of Single Walled Carbon Nanotubes: The Problem with Oxidation Debris. *Chem. Phys. Lett.* **2008**, *460*, 162–167.
33. Peng, X. J.; Jia, J. J.; Gong, X. M.; Luan, Z. K.; Fan, B. Aqueous Stability of Oxidized Carbon Nanotubes and the Precipitation by Salts. *J. Hazard. Mater.* **2009**, *165*, 1239–1242.
34. Smith, B.; Wepasnick, K.; Schrote, K. E.; Bertele, A. H.; Ball, W. P.; O'Melia, C.; Fairbrother, D. H. Colloidal Properties of Aqueous Suspensions of Acid-Treated, Multi-Walled Carbon Nanotubes. *Environ. Sci. Technol.* **2009**, *43*, 819–825.
35. Salvador-Morales, C.; Flahaut, E.; Sim, E.; Sloan, J.; Green, M. L. H.; Sim, R. B. Complement Activation and Protein Adsorption by Carbon Nanotubes. *Mol. Immunol.* **2006**, *43*, 193–201.
36. Poland, C. A.; Duffin, R.; Kinloch, I.; Maynard, A.; Wallace, W. A.; Seaton, A.; Stone, V.; Brown, S.; Macnee, W.; Donaldson, K. Carbon Nanotubes Introduced into the Abdominal Cavity of Mice Show Asbestos-Like Pathogenicity in a Pilot Study. *Nature Nanotechnol.* **2008**, *3*, 423–428.
37. Becker, M. L.; Fagan, J. A.; Gallant, N. D.; Bauer, B. J.; Bajpai, V.; Hobbie, E. K.; Lacerda, S. H.; Migler, K. B.; Jakupciak, J. P. Length-Dependent Uptake of DNA-Wrapped Single-Walled Carbon Nanotubes. *Adv. Mater.* **2007**, *19*, 939–945.
38. Hu, H.; Yu, A. P.; Kim, E.; Zhao, B.; Itkis, M. E.; Bekyarova, E.; Haddon, R. C. Influence of the Zeta Potential on the Dispersability and Purification of Single-Walled Carbon Nanotubes. *J. Phys. Chem. B* **2005**, *109*, 11520–11524.
39. Wang, Z. W.; Shirley, M. D.; Meikle, S. T.; Whitby, R. L. D.; Mikhalovsky, S. V. The Surface Acidity of Acid Oxidised Multi-Walled Carbon Nanotubes and the Influence of *in-Situ* Generated Fulvic Acids on Their Stability in Aqueous Dispersions. *Carbon* **2009**, *47*, 73–79.
40. Derjaguin, B. V.; Landau, L. D. Theory of the Stability of Strongly Charged Lyophobic Sols and of the Adhesion of Strongly Charged Particles in Solutions of Electrolytes. *Acta Physicochim. URSS* **1941**, *14*, 733–762.
41. Verwey, E. J. W. Theory of the Stability of Lyophobic Colloids. *J. Phys. Chem.* **1948**, *51*, 631–636.
42. McPhail, M. R.; Sells, J. A.; He, Z.; Chusuei, C. C. Charging Nanowalls: Adjusting the Carbon Nanotube Isoelectric Point *via* Surface Functionalization. *J. Phys. Chem. C* **2009**, *113*, 14102–14109.
43. Jiang, J. K.; Oberdorster, G.; Biswas, P. Characterization of Size, Surface Charge, and Agglomeration State of Nanoparticle Dispersions for Toxicological Studies. *J. Nanopart. Res.* **2009**, *11*, 77–89.
44. Mosmann, T. Rapid Colorimetric Assay for Cellular Growth and Survival—Application to Proliferation and Cytotoxicity Assays. *J. Immunol. Methods* **1983**, *65*, 55–63.
45. Wörle-Knirsch, J. M.; Pulskamp, K.; Krug, H. F. Oops They Did It Again! Carbon Nanotubes Hoax Scientists in Viability Assays. *Nano Lett.* **2006**, *6*, 1261–1268.
46. Cui, D. X.; Tian, F. R.; Ozkan, C. S.; Wang, M.; Gao, H. J. Effect of Single Wall Carbon Nanotubes on Human Hek293 Cells. *Toxicol. Lett.* **2005**, *155*, 73–85.
47. Kaiser, J. P.; Wick, P.; Manser, P.; Spohn, P.; Bruinink, A. Single Walled Carbon Nanotubes (SWCNT) Affect Cell Physiology and Cell Architecture. *J. Mater. Sci., Mater. Med.* **2008**, *19*, 1523–1527.
48. Zeineldin, R.; Al-Haik, M.; Hudson, L. G. Role of Polyethylene Glycol Integrity in Specific Receptor Targeting of Carbon Nanotubes to Cancer Cells. *Nano Lett.* **2009**, *9*, 751–757.
49. Cherkasova, A. S.; Shan, J. W. Impact of Altering Aspect Ratio of the Loading Particles on a Suspension's Thermal Conductivity. *Proc. IMECE 2008: Heat Transfer, Fluid Flows, Therm. Syst.* **2009**, *10*, 1979–1989.